

Beyond resource selection: emergent spatio-temporal distributions from animal movements and stigmergent interactions

Jonathan R. Potts^{1,a}, Valeria Giunta¹, Mark A. Lewis²

1 School of Mathematics and Statistics, University of Sheffield, Hicks Building, Hounsfield Road, Sheffield, S3 7RH, UK

2 Department of Mathematical and Statistical Sciences and Department of Biological Sciences, University of Alberta, Edmonton T6G 2G1, Alberta, Canada

a Corresponding author. Email: j.potts@sheffield.ac.uk; Tel: +44(0)114-222-3729

Abstract

A principal concern of ecological research is to unveil the causes behind observed spatio-temporal distributions of species. A key tactic is to correlate observed locations with environmental features, in the form of resource selection functions or other correlative species distribution models. In reality, however, the distribution of any population both affects and is affected by those surrounding it, creating a complex network of feedbacks causing emergent spatio-temporal features that may not correlate with any particular aspect of the underlying environment. Here, we study the way in which the movements of populations in response to one another can affect the spatio-temporal distributions of ecosystems. We construct a stochastic individual-based modelling (IBM) framework, based on stigmergent interactions (i.e. organisms leave marks which cause others to alter their movements) between and within populations. We show how to gain insight into this IBM via mathematical analysis of a partial differential equation (PDE) system given by a continuum limit. We show how the combination of stochastic simulations of the IBM and mathematical analysis of PDEs can be used to categorise emergent patterns into homogeneous vs. heterogeneous, stationary vs. perpetually-fluctuating, and aggregation vs. segregation. In doing so, we develop techniques for understanding spatial bifurcations in stochastic IBMs, grounded in mathematical analysis. Finally, we demonstrate

through a simple example how the interplay between environmental features and between-population stigmergent interactions can give rise to predicted spatial distributions that are quite different to those predicted purely by accounting for environmental covariates.

Key words: animal movement, animal space use, individual based models, partial differential equations, resource selection, species distribution models, stigmergy

1 Introduction

Understanding the processes behind the spatial distributions of animal populations has been a core concern of ecological research throughout its history (Elton, 2001; Nathan *et al.*, 2008). Today, the need to manage the effects of rapid anthropogenic actions on ecosystems makes predictive tools for spatial ecology more important than ever (Azaele *et al.*, 2015; Maris *et al.*, 2018). However, spatial ecology is complicated by the fact that the distribution of a population of organisms will affect the distributions of those populations that surround it, and also be affected by these populations (Morales *et al.*, 2010; Ovaskainen & Abrego, 2020). This generates a complex network of feedbacks between the constituent populations of an ecosystem, causing spatio-temporal patterns that can be difficult to predict, and impossible without the correct mathematical and computational tools linking process to pattern (May, 2019; Potts & Lewis, 2019).

There are two principal processes by which space use can be affected by interactions between populations (we use the word ‘population’ loosely, referring to anything ranging from a small group such as a territorial unit or herd through to an entire species). First, interactions can affect *demographics*, i.e. birth- and death-rates. This can be, for example, through predator-prey interactions or competition for resources, both of which are well-known to have non-trivial effects on both the overall demographic dynamics and the spatial distribution of species (Holmes *et al.*, 1994; Tilman *et al.*, 1997; Okubo & Levin, 2001; Cantrell & Cosner, 2004; Lewis *et al.*, 2013, 2016).

Second, for mobile organisms, population interactions can affect the *movement* of individuals (Mitchell & Lima, 2002; Vanak *et al.*, 2013; Breed *et al.*, 2017; Matthews *et al.*, 2020). It is well-known, from the mathematical literature, that the two processes of demographics and movement can combine to affect spatial distribution patterns in non-trivial ways, as exemplified by studies of cross-diffusion and prey-taxis (Shigesada *et al.*, 1979; Lee *et al.*, 2009; Gambino *et al.*, 2013; Potts & Petrovskii, 2017; Han & Dai, 2019; Haskell & Bell, 2020). These studies typically model movement and demographics in the same system of equations (usually partial differential equations), implying that the movements are occurring on the same spatio-temporal scale as the demographics. Therefore the movements considered in such studies are usually dispersal events. However, many animal populations can make significant movements to rearrange themselves in space over timescales where births and deaths are negligible (Moorcroft *et al.*, 2006; Vanak *et al.*, 2013; Ellison *et al.*, 2020). This particularly applies to larger animals, such as birds, mammals, and reptiles, who have great capability for movement but may only reproduce at a particular time of the year (e.g. spring). Therefore it is important to understand how movement processes alone may affect spatio-temporal population patterns (Potts & Lewis, 2019).

Spurred by rapid improvements in animal tagging technology, the empirical study of movement has surged, with data being gathered at ever higher resolutions (Williams *et al.*, 2020). Furthermore, an increasing number of studies are measuring animal interactions via the co-tagging of multiple animals and new techniques for decoding the resulting information (Vanak *et al.*, 2013; Potts *et al.*, 2014c; Schlägel *et al.*, 2019). A key goal of movement ecology is to understand animal space use, so the question of how fine-grained movement and interaction processes upscale to broader spatio-temporal patterns is gaining significant methodological attention (Avgar *et al.*, 2016; Signer *et al.*, 2017; Potts & Schlägel, 2020). However, to make predictions requires a theoretical understanding of how movements mediated by between-population interactions affect space use. Our principal aim here is to provide the theoretical framework for answering such questions.

Mutual attraction:



Mutual avoidance:



Pursue-and-avoid:

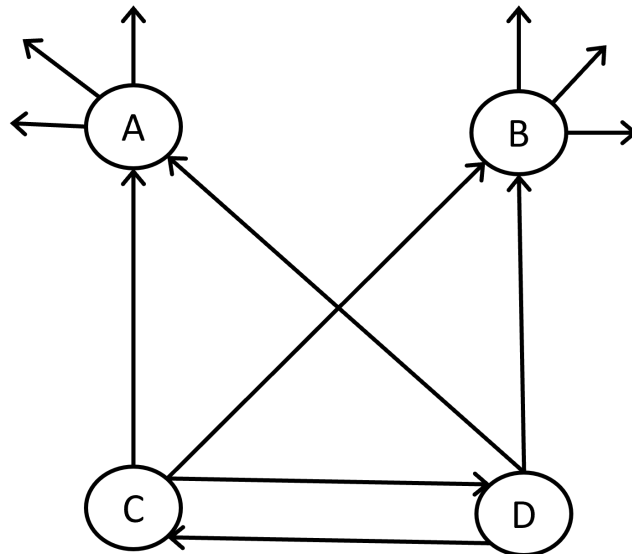
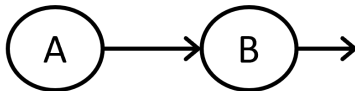


Fig. 1. Schematic diagram of stigmergent interactions. The left-hand side shows the three possible pairwise interactions between two populations. On the right is an example network built from these interactions. One might imagine that A and B are competing prey being predated by mutualistic predators C and D.

To this end, we construct a general and extensible individual-based model (IBM) of movements and interactions between multiple populations. We assume that animals, left alone on the landscape, will have some sort of movement process allowing them to embark on daily activities such as foraging. We model this very simply as a nearest-neighbour lattice random walk (Okubo & Levin, 2001; Codling *et al.*, 2008). This is a foundational movement model, which can be readily extended if one is interested in the finer details of foraging activity.

In this study, however, our focus is on the interactions between individuals and populations. For this, we assume that, as individuals move, they leave a trace of where they have been on the landscape, which could be in the form of scent, visual or olfactory marks, feces or a simply a trail. These marks decay over time if the area is not revisited. Consequently, each population leaves a distribution of such marks on the landscape, which changes over time as the constituent individuals move about. Individuals of a population alter their movement according to the presence or otherwise of marks, both from their own population and from others.

This process of leaving marks that cause others to alter their movement is called stigmergy, and has been studied in various contexts, including collective animal movement and territorial formation (Theraulaz & Bonabeau, 1999; Giuggioli *et al.*, 2013; White *et al.*, 2020). For any given pair of populations, A and B , one could either have mutual avoidance (where individuals from A avoid the marks of B and B avoid those of A), mutual attraction (individuals from A and B are attracted to the marks of one another), or pursuit-and-avoidance (individuals from A are attracted to marks of B but those from B avoid the marks of A). These combine into a network of stigmergent interactions that together determine the overall spatio-temporal distribution of the constituent populations (Figure 1). Our model is a generalisation of previous models of territory formation from stigmergent interactions (Giuggioli *et al.*, 2011, 2013; Potts *et al.*, 2012). However, these previous models were restricted to mutual avoidance processes and typically had only one individual per ‘population’ (recall, we are using ‘population’ quite generically here and could mean anything from a territorial unit to a larger group to a whole species, depending on context).

As well as stochastic simulation analysis, we also examine the continuum limit of our IBM model in space and time. We construct the IBM so that this limit is a system of partial differential equations (PDEs) studied previously in Potts & Lewis (2019). This formal connection between IBM and PDE enables us to use the mathematical tools of PDE analysis to gain insight into the expected behaviour of the IBM, which we can verify through simulation. The resulting techniques allow us to use PDE analysis as a starting-point for exploring IBM models. This is valuable because PDEs are amenable to mathematical analysis, enjoying a huge history of analytic techniques (Evans, 2010; Murray, 2012). However, IBMs are closer to reality and may be more amenable to extensions that incorporate further realism beyond what is studied here (for example, realistic movement processes based on life history needs such as foraging and tending to young). Such formal connections between IBMs and PDEs are powerful as they enable the best of both worlds: combining rigorous mathematical analysis with realistic modelling.

Finally, we explain how to account for landscape heterogeneity in our model, through coupling our IBM to a step selection function (Fortin *et al.*, 2005; Potts *et al.*, 2014a; Avgar *et al.*, 2016). We illustrate this with a simple example of two co-existing populations competing for the same resource, inspired by wolf-coyote coexistence in the Greater Yellowstone Ecosystem (Arjo & Pletscher, 2000). We investigate how the inclusion of interactions between and within the populations combine with the heterogeneous landscape. We show how this combination can cause emergent spatio-temporal patterns that cannot be explained merely by examining the effect of landscape heterogeneity on animal space use (as is the norm in resource selection studies and many other species distribution models).

Overall, our study aims to provide both insights into the effect of stigmergent interactions between populations on the spatio-temporal distribution of mobile species, and provide extensible methods for studying these emergent features. This complements the burgeoning statistical field of joint species distribution modelling, which gives tools for inferring the effect of one (or more) species on the distribution of another (Ovaskainen & Abrego, 2020), whilst also enhancing this field by demonstrating the importance of considering the nonlinear feedbacks between the movement processes of constituent populations for understanding spatial distributions.

2 Methods

2.1 The model

Our model of animal movement and stigmergent interactions is based on a nearest-neighbour lattice random walk formalism. We work on an $L \times L$ square lattice, Λ . We choose periodic boundary conditions for simplicity of presentation, although other forms are possible. We assume that there are N populations and that, for each index $i = 1, \dots, N$, population i consists of M_i individuals. Individuals leave marks at each lattice site they visit, and those marks decay geometrically over time. For simplicity, one can think of these marks as scent, such as faeces or urine, but they could correspond to any form by which animals may leave a trace of their

presence on the environment. The movement of each individual is biased by the presence of marks from both their own population and others. For each population, this bias could be either attractive or repulsive, depending on whether it is beneficial or detrimental for individuals of one population to be in the presence of another population. Since animals look at their surroundings at a distance to make movement decisions, our model allows for individuals to respond to the local average density of nearby marks.

Mathematically this situation can be described by writing down the probability $f(\mathbf{x}, t + \tau|\mathbf{x}', t)$ of moving from lattice site \mathbf{x}' to \mathbf{x} in a timestep of length τ . This function f is known as a *movement kernel*. To construct our movement kernel, we use a generalised linear model to describe the attraction to, or repulsion from, the local average density of nearby marks. A second equation is then required to describe how marks are averaged over space. Finally, the deposition and decay of marks over time is given by a third equation. We now give precise functional forms of these three equations in turn.

Letting l be the lattice spacing and $m_i(\mathbf{x}, t)$ be the density of marks from population i at location \mathbf{x} at time t , the movement kernel is given by

$$f(\mathbf{x}, t + \tau|\mathbf{x}', t) = \begin{cases} K_{\mathbf{x}'} \exp \left[\sum_{j=1}^N a_{ij} \bar{m}_j^\delta(\mathbf{x}, t) \right], & \text{if } |\mathbf{x} - \mathbf{x}'| = l, \\ 0, & \text{otherwise.} \end{cases} \quad (1)$$

Here $K_{\mathbf{x}'} = \sum_{\mathbf{x}} f(\mathbf{x}, t + \tau|\mathbf{x}', t)$ is a normalising constant ensuring that $f(\mathbf{x}, t + \tau|\mathbf{x}', t)$ is a well-defined probability distribution; if $a_{ij} > 0$ (resp. $a_{ij} < 0$) then $|a_{ij}|$ is the strength of population i 's attraction to (resp. repulsion from) population j ; and $\bar{m}_j^\delta(\mathbf{x}, t)$ represents the average mark density over a radius of δ .

The equation for this average mark density is

$$\bar{m}_j^\delta(\mathbf{x}, t) = \frac{1}{|S_\delta|} \sum_{\mathbf{z} \in S_\delta} m_j(\mathbf{x} + \mathbf{z}, t), \quad (2)$$

where $S_\delta = \{\mathbf{z} \in \Lambda : |\mathbf{z}| < \delta\}$ is the set of lattice sites that are within a distance of δ from 0

and $|S_\delta|$ is the number of lattice sites in S_δ .

The equation defining the change in marks over time, which are deposited by individuals and then decay geometrically, is

$$m_i(\mathbf{x}, t + \tau) = (1 - \mu_\tau)m_i(\mathbf{x}, t) + \rho_\tau \mathcal{N}_i(\mathbf{x}, t), \quad (3)$$

where $\mathcal{N}_i(\mathbf{x}, t)$ is the number of individuals at location \mathbf{x} in population i at time t , μ_τ is the amount by which marks decay in a time step of length τ , and ρ_τ is the amount of marking made by a single animal in a single time step.

Equations (1-3) are not the only available functional forms to describe our stigmergent process. However, the specific form for Equation (1) is advantageous because it arrives in the form of a step selection function (Fortin *et al.*, 2005; Avgar *et al.*, 2016). It thus has the potential to be parametrised by the methods of Schlägel *et al.* (2019), which deals with step selection for interacting individuals (although here we focus on analysing the emergent features of the model in Equation (3) rather than the question of fitting this model to data.) Equation (2) assumes that marks are averaged over a fixed disc around the individual and was chosen for simplicity, but other options, such as exponentially decaying averaging kernels, are also possible. Equation (3) was, likewise, chosen for simplicity. One drawback is that there, in theory, is no limit on the amount of marks in one location. If it is necessary to account for such a limit, one might exchange the $\rho_\tau \mathcal{N}_i(\mathbf{x}, t)$ term for something like $\rho_\tau(1 - \mathcal{N}_i(\mathbf{x}, t)/\mathcal{N}_{\max})\mathcal{N}_i(\mathbf{x}, t)$, where \mathcal{N}_{\max} is the maximum number of marks at a single location. However, we do not explore this extension in detail here; much insight can be gained without needing to incorporate this extra complexity.

2.2 Methods for analysing simulation output

We analyse the individual-based model (IBM) from Equations (1-3) using stochastic simulations. Example simulation runs reveal a range of patterns (Fig. 2). Here, we detail methods for characterising these via three broad questions: (I) Is the distribution of animal locations

heterogeneous or homogeneous? (II) If heterogeneous, do the patterns stabilise over time, so that populations keep broadly to fixed areas of space, or do they undergo persistent fluctuations? (III) For any two populations, are they segregated from one another or aggregated in the same small area? The stochastic nature of the IBM means that there will always be some amount of heterogeneity and persistent fluctuations due to noise. Our methods thus need to distinguish between what is noise and what is an actual pattern.

To answer question (I), we examine the local population density, $l_{i,d}(\mathbf{x}, t)$, averaged around a disc of radius d , at each lattice site x and time t , for each population i . At each point in time, we compute the *amplitude* of the pattern as $A_{i,d}(t) = \max_{\mathbf{x}}[l_{i,d}(\mathbf{x}, t)] - \min_{\mathbf{x}}[l_{i,d}(\mathbf{x}, t)]$, the maximum local population density across space minus the minimum. We want to find out whether the amplitude ever becomes higher than would be expected from individuals moving as independent random walkers (i.e. when $a_{ij} = 0$ for all i, j in Equation 1), assuming that the individuals are initially distributed uniformly at random on the lattice. For this, we calculate $A_{i,d}(t)$ in the case $a_{ij} = 0$ for all i, j (i.e. no mark deposition so no interactions between walkers) and take the average over a sufficiently long time period to calculate the mean to a given degree of accuracy (i.e. so that the standard deviation of the mean is below a pre-defined threshold, determined by the needs of the simulation experiment). We call this mean amplitude A_{rw} (for ‘random walk’). Then the extent to which the patterns are heterogenous can be determined with reference to this base-line value.

Question (II) requires that we keep track of the mean location of individuals in each population. Since individuals are moving on a lattice with periodic boundary conditions, it is necessary to take a circular mean (Berens, 2009). However, if individuals are roughly uniformly spread in either the horizontal or vertical direction then the circular mean can be very sensitive to stochastic fluctuations. We therefore introduce a *corrected circular mean* which accounts for this, and denote it by $\mathbf{c}_i(t)$ (notice that this is a location in two dimensions, for each time, t). Precise details of how to calculate $\mathbf{c}_i(t)$ are given in Supplementary Appendix A.

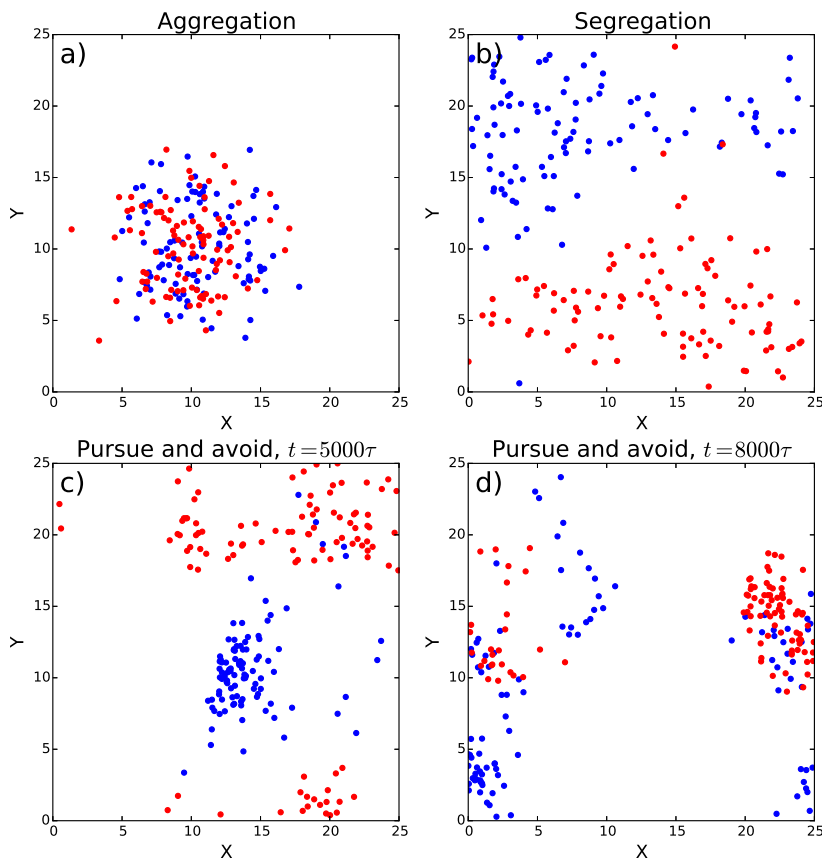


Fig. 2. Example snapshots of simulation output. In all panels, two populations of 100 individuals each were simulated on a 25×25 lattice, with initial locations distributed uniformly at random on the landscape. Also $\mu = 0.001$ and $\rho = 0.01$ for all panels (Equation 3). Panel (a) shows a system where two populations form a single, stable aggregation. Here, $a_{11} = a_{22} = 0$, $a_{12} = a_{21} = 2$, $\delta = 10l$ (Equation 1). In panel (b) the populations segregate into distinct parts of space. Here, $a_{11} = a_{22} = 0$, $a_{12} = a_{21} = -2$, and $\delta = 5l$. In both Panels (a) and (b) the snapshot is taken at time $t = 5000\tau$. Panels (c) and (d) show a situation where one population (blue) chases other (red) around the landscape in perpetuity, with snapshots at two different times. Here, $a_{11} = a_{22} = 1$, $a_{12} = 10$, $a_{21} = -10$, and $\delta = 10l$.

As with the amplitude calculations, we need to determine whether changes in $\mathbf{c}_i(t)$ are indicative of a fluctuating pattern (like in Figs. 2c,d) or just noise around an essentially stationary population distribution (as in Figs. 2a,b). For any length R and time-interval, T ,

we say that a system has become (R, T) -stable at time T_* if $|\mathbf{c}_i(T_* + t) - \mathbf{c}_i(T_*)| < R$ for each population i whenever $0 \leq t \leq T$. For example, the systems in Figs. 2a,b are both $(l, 1000\tau)$ -stable, but the system shown in Figs. 2c,d is not. In Section 2.3 we will show how to choose values of R and T , by ensuring they are consistent with the results of mathematical analysis.

For Question (III), the extent to which a pair of populations i, j ($i \neq j$) is aggregated or segregated at any point in time is measured using the *separation index*, $s_{ij}(t) = |\mathbf{c}_i(t) - \mathbf{c}_j(t)|$. For systems that become (R, T) -stable at some time T_* , we can define the asymptotic separation index s_{ij}^* as the average of $s_{ij}(t)$ across $T_* < t < T_* + T$. A separation index close to 0 indicates that the populations are occupying a similar part of space. If we know, from Question (I), that both populations are displaying heterogeneous patterns then in this case we have an aggregation of both populations. Higher separation indices, coupled with the existence of heterogeneous patterns, are suggestive of segregation patterns.

The separation index is a simple metric that is quick to calculate for multiple simulation analysis. However, one could also use more sophisticated measures of range overlap, such as the Bhattacharyya's Affinity (Fieberg & Kochanny, 2005) between kernel density estimators (Worton, 1989; Fleming *et al.*, 2015). Here, though, we will keep things simple, to enable analysis of a broader range of simulation scenarios in a realistic time-frame.

2.3 Mathematical techniques

Techniques for analysing the output of stochastic IBMs can involve choices that might be somewhat arbitrary, for example the choices of T_{amp} , R , and T in Section 2.2. Therefore it is valuable to ground-truth these choices by means of mathematical analysis. In particular, we do this via a PDE approximation describing the probability distribution of individuals for each population. In PDE theory, patterns can emerge when a change in parameter causes the system to switch from a situation whereby the constant steady state (corresponding to homogeneously distributed individuals) becomes unstable, leading to the distribution tending to either a non-constant steady state (heterogeneously distributed individuals), or entering a

perpetually fluctuating situation. The parameter value where the switch occurs is called a bifurcation point. The nature of this bifurcation point can be ascertained by a combination of linear stability analysis (LSA) and weakly non-linear analysis. Here we focus on LSA for simplicity (which is also called Turing pattern analysis, after Turing (1952)).

To arrive at a PDE system, we take a continuous limit in both space and time, sending l and τ to 0 such that l^2/τ tends to a finite constant, $D > 0$. This is sometimes called the diffusion limit, as D is a diffusion constant, but is also referred to as the parabolic limit (Hillen & Painter, 2013). If we take this limit, and also assume that infinitesimal moments beyond the second are negligible, we arrive at the following system of PDEs (see Supplementary Appendix B for details)

$$\frac{\partial u_i}{\partial t} = \underbrace{D\nabla^2 u_i}_{\text{Diffusive movement}} - \underbrace{2D\nabla \cdot \left[u_i \nabla \sum_{j=1}^N a_{ij} \bar{q}_j^\delta \right]}_{\text{Advection due to presence of marks}}, \quad (4)$$

$$\frac{\partial q_i}{\partial t} = \underbrace{\rho u_i}_{\text{Mark deposition}} - \underbrace{\mu q_i}_{\text{Mark decay}}, \quad (5)$$

for each $i = 1, \dots, N$, where $u_i(\mathbf{x}, t)$ is the location density of population i , $q_i(\mathbf{x}, t)$ is the density of marks, ρ is the limit of $\frac{\rho\tau}{\tau}$ as $\rho\tau, \tau \rightarrow 0$, μ is the limit of $\frac{\mu\tau}{\tau}$ as $\mu\tau, \tau \rightarrow 0$, and $\bar{q}_j^\delta(\mathbf{x}, t)$ is the average of $q(\mathbf{x}, t)$ over a ball of radius δ . It is sometimes helpful to simplify calculations by assuming that q_i equilibrates much faster than u_i , so that the scent mark is in quasi-equilibrium ($\frac{\partial q_i}{\partial t} = 0$), leading to the following equation for each $i = 1, \dots, N$

$$\frac{\partial u_i}{\partial t} = D\nabla^2 u_i - \frac{2D\rho}{\mu} \nabla \cdot \left[u_i \nabla \sum_{j=1}^N a_{ij} \bar{q}_j^\delta \right]. \quad (6)$$

The LSA technique enables us to use Equations (4-5) to construct the *pattern formation matrix*, \mathcal{M} (see Supplementary Appendix C for the full expression and derivation). The eigenvalues of \mathcal{M} give key information about whether heterogeneous patterns will spontaneously form from

small perturbations of a homogeneous system (i.e. individuals initially uniformly distributed on the landscape), and also whether these patterns begin to oscillate as they emerge.

The emergence of heterogeneous patterns is expected whenever there is an eigenvalue whose real part is positive. Thus the sign of the eigenvalue with biggest real part (a.k.a. the dominant eigenvalue) gives an indication of the answer to Question (I) above. If the dominant eigenvalue has positive real part and a non-zero imaginary part then small perturbations of the homogeneous system will oscillate as they grow, at least at small times. Often (but not always) these oscillations will persist for all times, so give an indication of the likely answer to Question (II). We stress that this is just an indication, though, and that discrepancies may exist between the answer to (II) and whether or not the dominant eigenvalue of \mathcal{M} is real. Full analysis of when to expect non-constant stationary patterns in Equation (4-5), or when to expect perpetually changing patterns, requires more sophisticated techniques.

2.4 Simulation experiments

To give some insight into the sort of patterns that can emerge from our model (Equations 1-3), we perform a variety of simulations in the simple case of two populations ($N = 2$). Throughout, we assume that each population has 100 individuals ($M_1 = M_2 = 100$) and we work on a 25×25 lattice. We assume $\tau = 1$ and $l = 1$ so can write $\mu_\tau = \mu$ and $\rho_\tau = \rho$ for ease of notation. We also assume $\delta = 5$ throughout.

First, we examine the situation where populations have a symmetric response to one another, so that $a_{12} = a_{21} = a$. For simplicity, we set $a_{11} = a_{22} = 0$. In this case the continuum limit PDE system (Equations 4-5) has the following pattern formation matrix (derived in Sup-

plementary Appendix C)

$$\mathcal{M} = \begin{pmatrix} -\kappa^2 & 0 & 0 & \frac{8a}{25}\kappa^2 \\ 0 & -\kappa^2 & \frac{8a}{25}\kappa^2 & 0 \\ \rho & 0 & -\mu & 0 \\ 0 & \rho & 0 & -\mu \end{pmatrix}. \quad (7)$$

Here, κ is the wavenumber of the patterns that may emerge at small times, if there is an eigenvalue of \mathcal{M} with positive real part (i.e. the wavelength of these patterns would be $2\pi/\kappa$). For our simulation experiments, we fix the scent-marking rate $\rho = 0.01$ to be a low number and vary the decay rate μ . We consider two different values of a : either $a = 2$, which corresponds to populations having a mutual attraction, or $a = -2$, corresponding to mutual avoidance. In either case, the dominant eigenvalue of \mathcal{M} is always real (Supplementary Appendix C). Furthermore, it is positive if and only if $\mu < 0.0064$. In other words, this mathematical analysis predicts that the system will bifurcate at $\mu = 0.0064$ from homogeneous patterns ($\mu > 0.0064$) to heterogeneous patterns ($\mu < 0.0064$). In other words, the heterogeneous patterns require that the decay rate of scent marks is sufficiently low so that the scent marks can accumulate and thereby substantially affect the movement behaviour.

To test whether we see a similar change in stability in simulations, we start by simulating our system in the case $\mu = 0.009$, run this until it is (R, T) -stable for $R = 1$ and $T = 1000$ and measure the asymptotic amplitude, $A_{i,d}^*$ for $i = 1, 2$, by averaging $A_{i,d}(t)$ over the 10000 time steps after (R, T) -stability has been achieved. For this, we use $d = 5$. We then use the final locations of each individual as initial conditions in our next simulation run, which is identical except for choosing $\mu = 0.0069$. We iterate this process, reducing μ by 0.0001 each time, until $\mu = 0.001$. This mimics the numerical bifurcation analysis often performed when analysing PDEs (Painter & Hillen, 2011). We perform this whole iterative process for both $a = 2$ and $a = -2$, the expectation being that $A_{i,d}^*$ will be approximately the same as that of non-interacting individuals (A_{rw}) until the value of μ crosses $\mu = 0.0064$, at which point we

expect $A_{i,d}^*$ to start increasing.

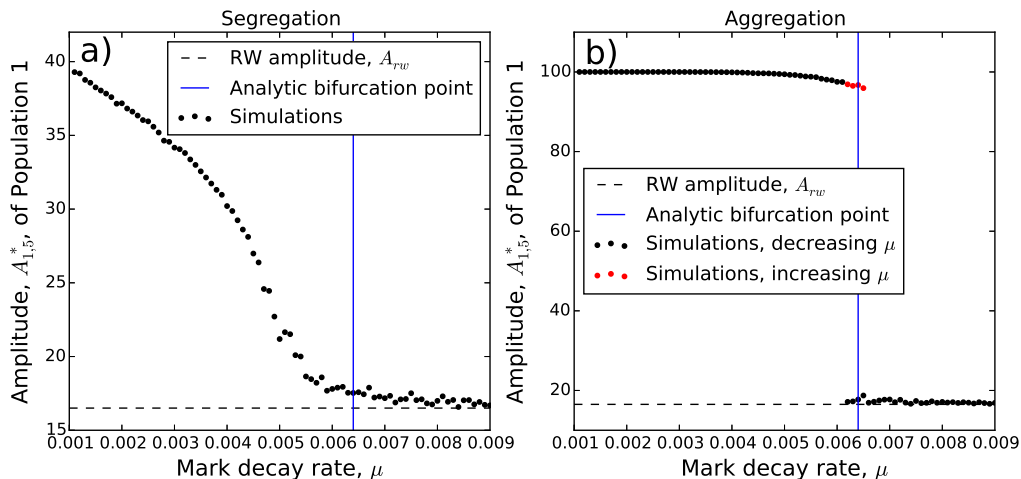


Fig. 3. Pattern formation analysis of stochastic simulations for $N = 2$. Each panel shows, using solid dots, the amplitude, $A_{1,5}^*$, of Population 1 for different values of μ , where $\rho = 0.01$, $a_{12} = a_{21} = a$, and $a_{11} = a_{22} = 0$. Black dots represent the situation where μ is decreased progressively (see Section 2.4 for details) and red dots show the situation where μ is increased (Section 3). In Panel (a), $a = -2$ so that the populations repel one another and in Panel (b), $a = 2$ so populations are attractive. The value A_{rw} , the amplitude in the situation where each individual is a non-interacting random walker, is given by the dashed black line. The blue line gives the bifurcation point predicted by analysis of the continuum limit PDE, Equations (4)-(5), which gives an indication of where we expect the amplitudes of the simulations to become notably larger A_{rw} .

To investigate whether linear stability analysis of the PDE system (Equations 4-5) reflects our method for answering Question (II), we set $a_{11} = a_{22} = 1$, $\rho = 0.01$, $\mu = 0.002$, and sample a_{12} and a_{21} uniformly at random, 100 times each, from the interval $[-5, 5]$. To make calculations more transparent, we assume that the scent marks are in quasi-equilibrium, taking the adiabatic approximation in Equation (6). In this case the pattern formation matrix is

$$\mathcal{M} = \frac{1}{5} \begin{pmatrix} 3 & 8a_{12} \\ 8a_{21} & 3 \end{pmatrix}, \quad (8)$$

and so the dominant eigenvalue is $(15 + 4\sqrt{a_{12}a_{21}})/25$. If the cross interaction terms are of identical sign ($a_{12}a_{21} > 0$) then linear stability analysis predicts stationary patterns to emerge

(at least at small times), but if they are of different sign ($a_{12}a_{21} < 0$) then the dominant eigenvalue is not real, so patterns should oscillate as they emerge. The latter case corresponds to the type of pursuit-and-avoidance situation that we see in Fig. 2c,d. We compare these predictions to our definition of (R, T) -stability for a range of values of R and T to ascertain the extent to which the separation between real and non-real eigenvalues corresponds to the existence or not of (R, T) -stability.

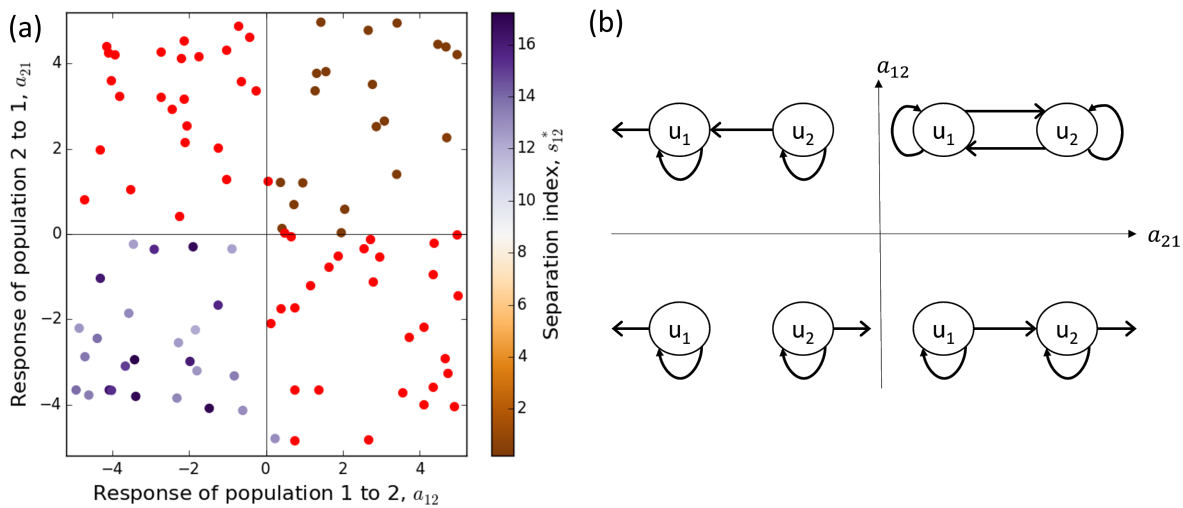


Fig. 4. Stability of emergent patterns. In Panel (a), each dot represents a simulation run of the IBM in Equations (1)-(3) where $a_{11} = a_{22} = 1$, $\rho = 0.01$, $\mu = 0.002$ and the values of a_{12} and a_{21} are given by the horizontal and vertical axes respectively. Red dots denote simulation runs that were not (R, T) -stable (for $R/l = 1$, $T/\tau = 7500$), whereas those on the purple-to-brown spectrum were (R, T) -stable. This colour spectrum corresponds to the separation index, from aggregative to segregative. Linear pattern formation analysis of the PDEs in Equations (4)-(5) predicts stationary (resp. non-stationary) patterns to emerge in the top-right and bottom-left (resp. top-left and bottom-right) quadrants, which corresponds well with the dot colours. Notice that the top-right (resp. bottom-left) quadrant corresponds to mutual attraction (resp. avoidance) and, likewise, the dot colours indicate aggregation (resp. segregation) patterns. Panel (b) gives a schematic of the between-population movement responses corresponding to the four quadrants in panel (a). An arrow from u_i to u_j represents attraction of population i towards population j . An arrow pointing out of u_i away from u_j represents u_i avoiding u_j .

R/l	T/τ	Agreement	SU/AS	SS/AU
0.5	5000	54%	46%	0%
1	5000	87%	0%	13%
1	7000	96%	0%	4%
1	7500	97%	2%	1%
1	8000	95%	5%	0%
2	5000	84%	0%	14%
2	7000	93%	0%	7%
2	7500	95%	0%	5%
2	8000	96%	4%	0%

Table 1. Extent to which analytic predictions agree with our simulation analysis for different choices of R and T . The third column gives the percentage of the simulations from Fig. 4 for which the analytic prediction for stability agrees with that measured from stochastic simulations using our method. The fourth (resp. fifth) gives the percentage for which the stochastic simulations were deemed unstable (resp. stable), for the given values of R and T , but the analytic prediction is stable (resp. unstable), denoted as SU/AS (rep. SS/AU).

2.5 Incorporating environmental effects

As mentioned at the end of Section 2.1, Equation (1) is in the form of a step selection function. This means that it can be readily used to incorporate the effect on movement of environmental or landscape features. Suppose that we have n such features, denoted by functions $Z_1(\mathbf{x}), \dots, Z_n(\mathbf{x})$. For each $k = 1, \dots, n$, denote by β_k the relative effect of $Z_k(\mathbf{x})$ on movement. Then, to incorporate these into the movement kernel, we modify Equation (1) as follows

$$f(\mathbf{x}, t + \tau | \mathbf{x}', t) = \begin{cases} K_{\mathbf{x}'} \exp \left[\sum_{j=1}^N a_{ij} \bar{m}_j^\delta(\mathbf{x}, t) + \sum_{k=1}^n \beta_k Z_k(\mathbf{x}) \right], & \text{if } |\mathbf{x} - \mathbf{x}'| = l, \\ 0, & \text{otherwise.} \end{cases} \quad (9)$$

We use this to investigate the effect on space use of interactions both between populations and with the environment, by considering a simple toy scenario, but one that is based on a particular empirical situation. Specifically, we consider two populations competing for the same heterogeneously-distributed resource, $Z_1(\mathbf{x})$ (here, $n = 1$). One population is assumed to be a weaker competitor, so avoids the stronger competitor, whilst the movements of the stronger are not affected by the weaker. Both have a tendency to move towards areas of higher-density

resources.

In our simulations, each population consists of 100 individuals. We examine three cases. The first is where the effect of the stronger competitor on the weaker is ignored (so animals are assumed to act independently, which mirrors many basic resource/step selection studies). The second incorporates the effect of the stronger on the weaker's movements, but treats each individual within a population as independent from the others in the population. This mirrors some recent resource selection studies whereby the movement of one population is affected by the presence of another, e.g. Vanak *et al.* (2013); Latombe *et al.* (2014). The third assumes that the stronger population are highly territorial, so are split into five separate sub-groups, each of which exhibit strong intra-group attraction but inter-group repulsion. The simulated resource layer is a Gaussian random field on a 25×25 lattice, previously used in the context of resource selection by (Potts *et al.*, 2014b). Precise details of the simulation experiments we performed are given in Supplementary Appendix D.

Whilst this situation is a deliberately general and simplified model, it is inspired by the particular situation of wolf-coyote coexistence in the Greater Yellowstone Ecosystem. Here, the stronger competitor is the wolf population, coyotes being weaker, and the resource layer is the distribution of where prey are likely to be found. The ability for coyotes to coexist with wolves in this system has been conjectured to emerge from the territorial structures of wolves, which include relatively large interstitial regions that may be havens for coyote (Arjo & Pletscher, 2000). If true, this means that the intra-pack attraction and inter-pack avoidance mechanisms are key to understanding the space use of wolves and coyotes. The three models presented here can be viewed as testing how the different assumptions about wolf-coyote and wolf-wolf interactions might interface with resource selection to affect their space use distributions.

3 Results

Fig. 3 shows the results of pattern formation analysis of our IBM. The place at which the amplitude grows higher than that of random non-interacting individuals is reasonably close to

the bifurcation point predicted by linear stability analysis of the corresponding continuum PDE system. However, the latter occurs at a slightly lower value of μ than for the IBM indicating that a slightly lower decay rate of marks is necessary to overcome the stochastic effects and allow patterns to form. In other words, the stochasticity has a mild homogenising effect.

For negative a (recall $a = a_{12} = a_{21}$ in Equation 1), where we tend to see segregation patterns beyond the bifurcation point, the amplitudes $A_{1,5}^*$, represented by black dots, appear to grow steadily as μ is decreased (Fig. 3a). However, for positive a , there is a sudden jump in the amplitude between $\mu = 0.0062$ and $\mu = 0.0061$ (Fig. 3b). Such jumps in bifurcation diagrams can sometimes be accompanied by a hysteresis effect, whereby if the initial conditions contain patterns then the patterns may persist even in parameter regimes where they would not emerge spontaneously. To test this, we performed the same IBM pattern formation analysis as before, but this time starting with $\mu = 0.0004$ and increasing μ by 0.0001 each iteration (rather than decreasing as before). The red dots in Fig. 3b show that there is indeed hysteresis in the IBM system, whereby the system is bistable for $0.006 \lesssim \mu \lesssim 0.0065$, a phenomenon that has also been observed in single population aggregation models with differential equation formalisms (Potts & Painter, 2021).

Fig. 4 shows that (R, T) -stability corresponds well to the predictions of pattern formation analysis in the case where $R = l$ and $T = 5000\tau$. These were the best values of R and T we found from the ones tested, inasmuch as the results corresponded to the pattern formation analysis in the highest proportion of cases, N% (Table 1). Notice too that the mutually-avoiding populations (with $a_{12}, a_{21} < 0$) tend to have much higher separation indices, s_{12}^* , than the mutually attracting populations, as one would expect.

Fig. 5 shows the results of our three simulation experiments on a heterogeneous resource landscape. When we assume that there are no inter-population interactions then the resulting model predicts space-use patterns whereby both populations have very similar space use distributions (Fig. 5a). When we account for the avoidance of the weaker population by the stronger then the model predicts that the stronger population will live where the resources are

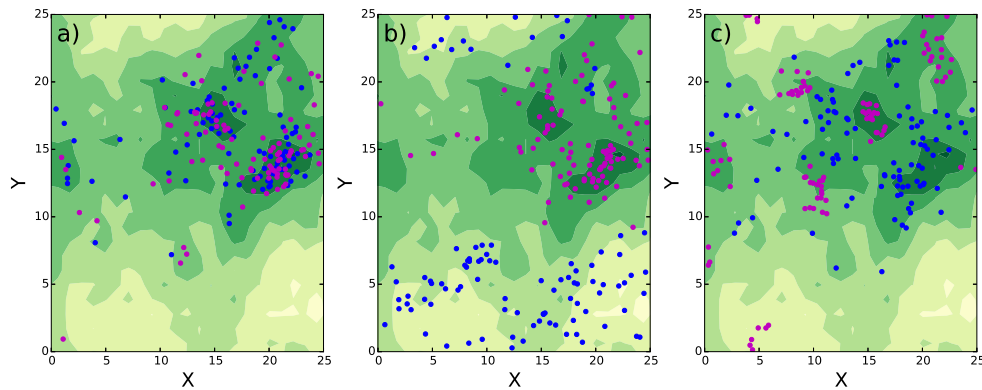


Fig. 5. Incorporating environmental effects. This figure shows the space use distributions that emerge from three different scenarios involving two populations attracted to the same heterogeneously-distributed resource. This resource is shown in shades of yellow-green, with darker (resp. lighter) green denoting higher (resp. lower) density of resources. Magenta (resp. blue) dots denote the stronger (resp. weaker) competitor. In Panel (a) the individuals do not alter their movement in response to the presence of others, and we simply see a preference for higher quality resources. In Panel (b), as well as attraction to better resources, the weaker (blue) population has a tendency to move away from the stronger (magenta) population. In addition to this avoidance mechanism, in Panel (c) the magenta population is strongly territorial. This leads to the emergence of interstitial regions where the blue population can access resources that may be quite high quality.

better, driving the weaker to resource-poor areas (Fig. 5b). This, of course, may ultimately lead to the weaker population being unable to survive. However, if the stronger population is strongly territorial, it can subdivide into separate groups, leaving interstitial regions where the weaker population can survive and have access to resources that may be relatively high quality (Fig. 5c).

4 Discussion

Resource selection analysis is one of the most popular techniques for understanding the distribution of species and populations. However, like many species distribution models, studies tend to focus on correlating animal locations with environmental and landscape features. Whilst some more recent studies in resource selection (Bastille-Rousseau *et al.*, 2015), step selection

(Vanak *et al.*, 2013), and species distribution modelling (Ovaskainen & Abrego, 2020) have examined the way presence of one population may affect that of another, the first population tends to be treated as a static layer, similar to a resource layer, which then affects the presence or movement of the second population. This assumption neglects the dynamic feedbacks that can occur between two or more populations of animals.

Here, we have shown that such feedbacks can generate a variety of emergent patterns that can be quite different to those that appear when only accounting for static layers (Fig. 5). We have given a basic categoration scheme for these patterns via simple binary questions: homogeneous or heterogeneous, stable or dynamic, segregated or aggregated. We have shown that, even with just two populations, all these patterns are possible. This categorisation, however, is likely to be only the tip of the iceberg in terms of the possible patterning properties arising from sigmoidal interactions between multiple populations. Indeed, a recent study of the limiting deterministic PDE (Potts & Lewis, 2019) unveiled a rich suite of patterns through numerical simulations, including all those patterns studied here, as well as period doubling bifurcations, travelling-waves, and irregular patterns suggestive of chaos. Whilst such subtleties in pattern formation may be tricky to distinguish from noise in an IBM, it is valuable to be aware that they may yet be present in real systems.

Whilst a coarse-grained, individual-based approach to ecological modelling is valuable in ensuring emergent phenomena are not simply an outcome of continuum assumptions (Durrett & Levin, 1994; Getz *et al.*, 2018), here the limiting PDE has been very valuable for gaining insight into our IBM. First, understanding the places where the PDE system bifurcates from between different patterning regimes has enabled us to identify interesting parameter regimes for studying our IBM (Figs. 3 and 4). Second, comparison between patterns in our IBM and the corresponding PDE has enabled us to tune the various otherwise-arbitrary choices of parameters used in analysing IBMs (e.g. the choices of R and T determined by Table 1). Whilst there is a tradition of ecological studies where limiting PDEs have helped decode the complexity inherent in IBMs (Durrett & Levin, 1994; Sherratt *et al.*, 1997; Hosseini, 2006), this

is perhaps overshadowed by the recent prevalence of IBM-only studies in ecology (Grimm, 1999; Grimm & Railsback, 2013; DeAngelis, 2018). We hope our use of PDEs here helps encourage further studies to implement PDEs as a tool for understanding IBMs.

Here, we have explored pattern formation analysis of PDEs using perhaps the simplest tool, that of linear analysis. However, there are plenty of other tools, with varying conceptual and mathematical complexity, that may provide insight. For example, in Fig. 3a, we see that patterns emerge smoothly as one decreases μ past the bifurcation point, which is suggestive of a super-critical bifurcation. However, in Fig. 3b, there is a sudden jump, together with a hysteresis (bistable) region, something usually accompanied by a sub-critical bifurcation. Techniques such as weakly non-linear analysis (Eftimie *et al.*, 2009) and Crandall-Rabinowitz abstract bifurcation theory (Buttenschön & Hillen, 2020) are able to distinguish rigorously between these two cases. These are, however, much more conceptually and technically demanding than linear analysis, and will require a significant, separate work.

On the more ecological side, we have shown how accounting for feedbacks between the movement mechanisms of constituent populations may help explain the emergence of interstitial regions in territorial animals that could provide safe-havens for weaker competitors. Such patterns have been observed in coexistent wolf and coyote populations in the Greater Yellowstone Ecosystem. There, these interstitial regions have also been observed as refuges for deer (Lewis & Murray, 1993). Although we did not consider the mobility of prey resources in our simple example, one could add extra complexity by considering the attempts of mobile prey to avoid predators, and observe how this affects the spatial patterns. However, for the purposes of our simple illustration, this level of modelling complexity was not required.

In general, our approach may be valuable for understanding the distribution of populations whenever the locations of two or more populations affect the movements of each other (Schlägel *et al.*, 2020). This has been observed in a variety of situations. We have already mentioned competition between carnivores, and indeed the movements of coexistent carnivore populations in response to the presence of others has been measured in various studies (Vanak *et al.*, 2013;

Swanson *et al.*, 2016). Also the effect of predator movement on prey locations (sometimes called prey-taxis), and vice versa (the ‘landscape of fear’), has been documented in a variety of scenarios (Kareiva & Odell, 1987; Laundré *et al.*, 2010; Latombe *et al.*, 2014; Gallagher *et al.*, 2017). Despite this, the predominant species distributions models used in ecology tend to not to account for the underlying between-population movement processes and the emergent features that they engender, even in cases where they model species jointly (Ovaskainen & Abrego, 2020). Explicit modelling of the underlying movement mechanisms, as we have done here, would help plug this gap and lead to more accurate description and forecasting of species distributions.

Acknowledgements

JRP and VG acknowledge support of Engineering and Physical Sciences Research Council (EPSRC) grant EP/V002988/1. MAL acknowledges support from the NSERC Discovery and Canada Research Chair programs.

References

1. Arjo, W.M. & Pletscher, D.H. (2000). Behavioral responses of coyotes to wolf recolonization in northwestern montana. *Canadian Journal of Zoology*, 77, 1919–1927.
2. Avgar, T., Potts, J.R., Lewis, M.A. & Boyce, M.S. (2016). Integrated step selection analysis: bridging the gap between resource selection and animal movement. *Methods Ecol. Evol.*, 7, 619–630.
3. Azaele, S., Maritan, A., Cornell, S.J., Suweis, S., Banavar, J.R., Gabriel, D. & Kunin, W.E.

- (2015). Towards a unified descriptive theory for spatial ecology: predicting biodiversity patterns across spatial scales. *Methods in Ecology and Evolution*, 6, 324–332.
4.
Bastille-Rousseau, G., Potts, J.R., Schaefer, J.A., Lewis, M.A., Ellington, E.H., Rayl, N.D., Mahoney, S.P. & Murray, D.L. (2015). Unveiling trade-offs in resource selection of migratory caribou using a mechanistic movement model of availability. *Ecography*, 38, 1049–1059.
5.
Berens, P. (2009). Circstat: a matlab toolbox for circular statistics. *Journal of Statistical Software*, 31, 1–21.
6.
Breed, G.A., Matthews, C.J., Marcoux, M., Higdon, J.W., LeBlanc, B., Petersen, S.D., Orr, J., Reinhart, N.R. & Ferguson, S.H. (2017). Sustained disruption of narwhal habitat use and behavior in the presence of arctic killer whales. *Proceedings of the National Academy of Sciences*, 114, 2628–2633.
7.
Buttenschön, A. & Hillen, T. (2020). Non-local cell adhesion models: Steady states and bifurcations. *arXiv preprint arXiv:2001.00286*.
8.
Cantrell, R.S. & Cosner, C. (2004). *Spatial ecology via reaction-diffusion equations*. John Wiley & Sons, Chichester.
9.
Codling, E.A., Plank, M.J. & Benhamou, S. (2008). Random walk models in biology. *J. Roy. Soc. Interface*, 5, 813–834.
- 10.

- DeAngelis, D.L. (2018). *Individual-based models and approaches in ecology: populations, communities and ecosystems*. CRC Press.
11.
Durrett, R. & Levin, S. (1994). The importance of being discrete (and spatial). *Theor. Pop. Biol.*, 46, 363–394.
12.
Eftimie, R., de Vries, G. & Lewis, M. (2009). Weakly nonlinear analysis of a hyperbolic model for animal group formation. *J. Math. Biol.*, 59, 37–74.
13.
Ellison, N., Hatchwell, B.J., Biddiscombe, S.J., J, N.C. & Potts, J.R. (2020). Mechanistic home range analysis reveals drivers of space use patterns for a non-territorial passerine. *Journal of Animal Ecology*, 89, 2763–76.
14.
Elton, C.S. (2001). *Animal ecology*. University of Chicago Press.
15.
Evans, L.C. (2010). *Partial differential equations*. American Mathematical Society, Providence, Rhode Island.
16.
Fieberg, J. & Kochanny, C.O. (2005). Quantifying home-range overlap: The importance of the utilization distribution. *The Journal of Wildlife Management*, 69, 1346–1359.
17.
Fleming, C.H., Fagan, W.F., Mueller, T., Olson, K.A., Leimgruber, P. & Calabrese, J.M. (2015). Rigorous home range estimation with movement data: a new autocorrelated kernel density estimator. *Ecology*, 96, 1182–1188.

18.

Fortin, D., Beyer, H., Boyce, M., Smith, D., Duchesne, T. & Mao, J. (2005). Wolves influence elk movements: Behavior shapes a trophic cascade in yellowstone national park. *Ecology*, 86, 1320–1330.

19.

Gallagher, A.J., Creel, S., Wilson, R.P. & Cooke, S.J. (2017). Energy landscapes and the landscape of fear. *Trends in Ecology & Evolution*, 32, 88–96.

20.

Gambino, G., Lombardo, M.C. & Sammartino, M. (2013). Pattern formation driven by cross-diffusion in a 2d domain. *Nonlinear Analysis: Real World Applications*, 14, 1755–1779.

21.

Getz, W.M., Marshall, C.R., Carlson, C.J., Giuggioli, L., Ryan, S.J., Romañach, S.S., Boettiger, C., Chamberlain, S.D., Larsen, L., D’Odorico, P. *et al.* (2018). Making ecological models adequate. *Ecology letters*, 21, 153–166.

22.

Giuggioli, L., Potts, J.R. & Harris, S. (2011). Animal interactions and the emergence of territoriality. *PLoS Computational Biology*, 7, e1002008.

23.

Giuggioli, L., Potts, J.R., Rubenstein, D.I. & Levin, S.A. (2013). Stigmergy, collective actions, and animal social spacing. *Proceedings of the National Academy of Sciences*, p. 201307071.

24.

Grimm, V. (1999). Ten years of individual-based modelling in ecology: what have we learned and what could we learn in the future? *Ecological modelling*, 115, 129–148.

25.

Grimm, V. & Railsback, S.F. (2013). *Individual-based modeling and ecology*. Princeton university press.

26.

Han, R. & Dai, B. (2019). Spatiotemporal pattern formation and selection induced by nonlinear cross-diffusion in a toxic-phytoplankton–zooplankton model with allee effect. *Nonlinear Analysis: Real World Applications*, 45, 822–853.

27.

Haskell, E.C. & Bell, J. (2020). Pattern formation in a predator-mediated coexistence model with prey-taxis. *Discrete & Continuous Dynamical Systems-B*, 25, 2895.

28.

Hillen, T. & Painter, K. (2013). Transport and anisotropic diffusion models for movement in oriented habitats. In: *Dispersal, Individual Movement and Spatial Ecology* (eds. Lewis, M.A., Maini, P.K. & Petrovskii, S.V.). Springer Berlin Heidelberg, Lecture Notes in Mathematics, pp. 177–222.

29.

Holmes, E.E., Lewis, M.A., Banks, J. & Veit, R. (1994). Partial differential equations in ecology: spatial interactions and population dynamics. *Ecology*, 75, 17–29.

30.

Hosseini, P.R. (2006). Pattern formation and individual-based models: the importance of understanding individual-based movement. *Ecological Modelling*, 194, 357–371.

31.

Kareiva, P. & Odell, G. (1987). Swarms of predators exhibit "prey taxis" if individual predators use area-restricted search. *The American Naturalist*, 130, 233–270.

32.

Latombe, G., Fortin, D. & Parrott, L. (2014). Spatio-temporal dynamics in the response of woodland caribou and moose to the passage of grey wolf. *Journal of Animal Ecology*, 83, 185–198.

33.

Laundré, J.W., Hernández, L. & Ripple, W.J. (2010). The landscape of fear: ecological implications of being afraid. *Open Ecology Journal*, 3, 1–7.

34.

Lee, J., Hillen, T. & Lewis, M. (2009). Pattern formation in prey-taxis systems. *J. Biol. Dynam.*, 3, 551–573.

35.

Lewis, M.A., Maini, P.K. & Petrovskii, S.V. (2013). Dispersal, individual movement and spatial ecology. *Lecture Notes in Mathematics (Mathematics Bioscience Series)*, 2071.

36.

Lewis, M.A. & Murray, J.D. (1993). Modelling territoriality and wolf-deer interactions. *Nature*, 366, 738–740.

37.

Lewis, M.A., Petrovskii, S.V. & Potts, J.R. (2016). *The mathematics behind biological invasions*. Springer, Switzerland.

38.

Maris, V., Huneman, P., Coreau, A., Kéfi, S., Pradel, R. & Devictor, V. (2018). Prediction in ecology: promises, obstacles and clarifications. *Oikos*, 127, 171–183.

39.

Matthews, C.J., Breed, G.A., LeBlanc, B. & Ferguson, S.H. (2020). Killer whale presence

- drives bowhead whale selection for sea ice in arctic seascapes of fear. *Proceedings of the National Academy of Sciences*, 117, 6590–6598.
40.
May, R.M. (2019). *Stability and complexity in model ecosystems*. Princeton university press.
41.
Mitchell, W.A. & Lima, S.L. (2002). Predator-prey shell games: large-scale movement and its implications for decision-making by prey. *Oikos*, 99, 249–259.
42.
Moorcroft, P.R., Lewis, M.A. & Crabtree, R.L. (2006). Mechanistic home range models capture spatial patterns and dynamics of coyote territories in yellowstone. *Proc. Roy. Soc. B*, 273, 1651–1659.
43.
Morales, J.M., Moorcroft, P.R., Matthiopoulos, J., Frair, J.L., Kie, J.G., Powell, R.A., Merrill, E.H. & Haydon, D.T. (2010). Building the bridge between animal movement and population dynamics. *Philosophical Transactions of the Royal Society B: Biological Sciences*, 365, 2289–2301.
44.
Murray, J.D. (2012). *Asymptotic analysis*. vol. 48. Springer Science & Business Media.
45.
Nathan, R., Getz, W.M., Revilla, E., Holyoak, M., Kadmon, R., Saltz, D. & Smouse, P.E. (2008). A movement ecology paradigm for unifying organismal movement research. *Proceedings of the National Academy of Sciences*, 105, 19052–19059.
46.
Okubo, A. & Levin, S.A. (2001). *Diffusion and ecological problems: modern perspectives*. vol. 14. Springer.

47.

Ovaskainen, O. & Abrego, N. (2020). *Joint species distribution modelling: with applications in R*. Cambridge University Press.

48.

Painter, K.J. & Hillen, T. (2011). Spatio-temporal chaos in a chemotaxis model. *Physica D: Nonlinear Phenomena*, 240, 363–375.

49.

Potts, J., Bastille-Rousseau, G., Murray, D., Schaefer, J. & Lewis, M. (2014a). Predicting local and non-local effects of resources on animal space use using a mechanistic step-selection model. *Methods Ecol. Evol.*, 5, 253–262.

50.

Potts, J.R., Auger-Méthé, M., Mokross, K. & Lewis, M.A. (2014b). A generalized residual technique for analysing complex movement models using earth mover's distance. *Methods in Ecology and Evolution*, 5, 1012–1022.

51.

Potts, J.R., Harris, S. & Giuggioli, L. (2012). Territorial dynamics and stable home range formation for central place foragers. *PLoS One*, 7, e34033.

52.

Potts, J.R. & Lewis, M.A. (2019). Spatial memory and taxis-driven pattern formation in model ecosystems. *Bull. Math. Biol.*, 81, 2725–2747.

53.

Potts, J.R., Mokross, K. & Lewis, M.A. (2014c). A unifying framework for quantifying the nature of animal interactions. *Journal of the Royal Society Interface*, 11, 20140333.

54.

- Potts, J.R. & Painter, K.J. (2021). Stable steady-state solutions of some biological aggregation models. *SIAM Journal on Applied Mathematics*, 81, 1248–1263.
- 55.
- Potts, J.R. & Petrovskii, S.V. (2017). Fortune favours the brave: Movement responses shape demographic dynamics in strongly competing populations. *J. Theor. Biol.*, 420, 190–199.
- 56.
- Potts, J.R. & Schlägel, U.E. (2020). Parametrizing diffusion-taxis equations from animal movement trajectories using step selection analysis. *Methods in Ecology and Evolution*, 11, 1092–105.
- 57.
- Schlägel, U.E., Grimm, V., Blaum, N., Colangeli, P., Dammhahn, M., Eccard, J.A., Hausmann, S.L., Herde, A., Hofer, H., Joshi, J. *et al.* (2020). Movement-mediated community assembly and coexistence. *Biological Reviews*, 95, 1073–1096.
- 58.
- Schlägel, U.E., Signer, J., Herde, A., Eden, S., Jeltsch, F., Eccard, J.A. & Dammhahn, M. (2019). Estimating interactions between individuals from concurrent animal movements. *Methods Ecol. Evol.*
- 59.
- Sherratt, J.A., Eagan, B.T. & Lewis, M.A. (1997). Oscillations and chaos behind predator–prey invasion: mathematical artifact or ecological reality? *Philosophical transactions of the Royal Society of London. Series B: Biological Sciences*, 352, 21–38.
- 60.
- Shigesada, N., Kawasaki, K. & Teramoto, E. (1979). Spatial segregation of interacting species. *Journal of theoretical biology*, 79, 83–99.

61.

Signer, J., Fieberg, J. & Avgar, T. (2017). Estimating utilization distributions from fitted step-selection functions. *Ecosphere*, 8, e01771.

62.

Swanson, A., Arnold, T., Kosmala, M., Forester, J. & Packer, C. (2016). In the absence of a “landscape of fear”: How lions, hyenas, and cheetahs coexist. *Ecology and evolution*, 6, 8534–8545.

63.

Theraulaz, G. & Bonabeau, E. (1999). A brief history of stigmergy. *Artificial life*, 5, 97–116.

64.

Tilman, D., Kareiva, P.M. *et al.* (1997). *Spatial ecology: the role of space in population dynamics and interspecific interactions*. Princeton University Press.

65.

Turing, A.M. (1952). The chemical basis of morphogenesis. *Phil. Trans. R. Soc. Lond. B*, 237, 37–72.

66.

Vanak, A., Fortin, D., Thakera, M., Ogdene, M., Owena, C., Greatwood, S. & Slotow, R. (2013). Moving to stay in place - behavioral mechanisms for coexistence of african large carnivores. *Ecology*, 94, 2619–2631.

67.

White, L.A., VandeWoude, S. & Craft, M.E. (2020). A mechanistic, stigmergy model of territory formation in solitary animals: Territorial behavior can dampen disease prevalence but increase persistence. *PLoS computational biology*, 16, e1007457.

68.

Williams, H.J., Taylor, L.A., Benhamou, S., Bijleveld, A.I., Clay, T.A., de Grissac, S.,

Demšar, U., English, H.M., Franconi, N., Gómez-Laich, A. *et al.* (2020). Optimizing the use of biologgers for movement ecology research. *Journal of Animal Ecology*, 89, 186–206.

69.

Worton, B.J. (1989). Kernel methods for estimating the utilization distribution in home-range studies. *Ecology*, 70, 164–168.